journal

Reprinted from the Journal of the American Ceramic Society, Vol. 78, No. 12, December 1995

J. Am. Ceram. Soc., 78 [12] 3369-75 (1995)

Effect of Fiber Volume Fraction on the Off-Crack-Plane Fracture Energy in Strain-Hardening Engineered Cementitious Composites

Mohamed Maalej, Toshiyuki Hashida,* and Victor C. Li

Advanced Civil Engineering Materials Research Laboratory, Department of Civil and Environmental Engineering, University of Michigan, Ann Arbor, Michigan 48109-2125

In this paper, the results of an experimental study on the effect of fiber volume fraction on the off-crack-plane fracture energy in a strain-hardening engineered cementitious composite (ECC) are presented. Unlike the well-known quasi-brittle behavior of fiber-reinforced concrete, ECC exhibits quasi-ductile response by developing a large damage zone prior to fracture localization. In the damage zone, the material is microcracked but continues to strain-harden locally. The areal dimension of the damage zone has been observed to be on the order of 1000 cm² in double cantilever beam specimens. The energy absorption of the off-crack-plane inelastic deformation process has been measured to be more than 50% of the total fracture energy of up to 34 kJ/m². This magnitude of fracture energy is the highest ever reported for a fiber cementitious composite.

I. Introduction

THREE types of fracture modes have been observed in cementitious materials (see Fig. 1 for a schematic illustration): brittle, quasi-brittle, and ductile. Brittle fracture mode can be observed in hardened cement paste material. It is characterized by a very small microcrack zone at the crack tip (Fig. 1(a)) typically of submillimeter scale, low fracture energy of the order of 0.01 kJ/m², and a linear load versus load point displacement (P–Δ) curve from a fracture test. Quasi-brittle fracture mode can be observed in concrete and in most fiber-reinforced cement or concrete (FRC). It is characterized by a bridging process zone in addition to the small microcrack zone at the crack tip (Fig. 1(b)). The bridging action provides additional energy absorption through aggregate and/or ligament bridging in concrete, and through fiber bridging in FRC, in the wake of the crack front. For quasi-brittle materials, the fracture energy extends over a large range, from 0.1 kJ/m² in concrete to several kJ/m² in the case of FRC. Correspondingly, the process zone size extends from millimeter scale to centimeter scale. The P–Δ curve from a fracture test may involve a small nonlinear region near the peak load with a significant postpeak tension-softening behavior. Ductile fracture mode has been recorded recently by Li and Hashida[1] in double cantilever beam (DCB) fracture specimens fabricated from a cement paste matrix reinforced with 2% by volume of polyethylene fibers. The recorded fracture behavior was characterized by the development of an off-crack-plane microcracked zone (as shown schematically in Fig. 1(c)) in addition to the bridging process zone observed in quasi-brittle fracture mode. The areal dimension of this inelastic damage zone was observed to be more than 500 cm², leading to an extensive off-crack-plane inelastic energy absorption. The total fracture energy consumed in the fiber bridging fracture process zone, and in the inelastically deformed material off the crack plane, was measured to be 24 kJ/m². The recorded P–Δ curve from the fracture test revealed an extended nonlinear region before reaching the peak load and a significant postpeak tension-softening behavior.

The ductile fracture phenomenon observed in the 2% polyethylene fiber composite was made possible by the strain-hardening behavior of the composite material. Compared to quasi-brittle materials, pseudo-strain-hardening materials are characterized by their ability to sustain higher levels of loading while undergoing large deformation under uniaxial tensile loading. When cementitious materials are properly reinforced with fibers, they can be made to exhibit pseudo-strain-hardening behavior accompanied by multiple parallel cracking. Pseudo-strain-hardening behavior has been demonstrated in continuous aligned[2,3] and discontinuous randomly distributed[1,4,5] fiber-reinforced cement materials. The conditions for pseudo-strain-hardening in the latter materials have recently been worked out based on micromechanics principles.[6–8] The resulting analytical tools have been used as guidelines for designing a number of strain-hardening engineered cementitious composites (ECCs).[4,5]

In the presence of a notch, some ECCs apparently have the ability to transfer the stress away from the notch tip and give rise to the development of microcrack damage. This process of strain delocalization gives the composite a macroscopically ductile fracture behavior, resulting in a highly damage-tolerant material. For such materials, the total energy J_c absorbed during fracture is, therefore, composed of two components. The first comes from the fiber pull-out process (bridging fracture energy J_b) on the main fracture plane, and the second comes from the microcracking process (off-crack-plane fracture energy J_m). The off-crack-plane fracture energy measured by Li and Hashida[1] for the 2% polyethylene fiber composite was about 50% of the total fracture energy. In this paper, the results of an experimental study on the effect of fiber volume fraction on the off-crack-plane fracture energy are presented. The experimental

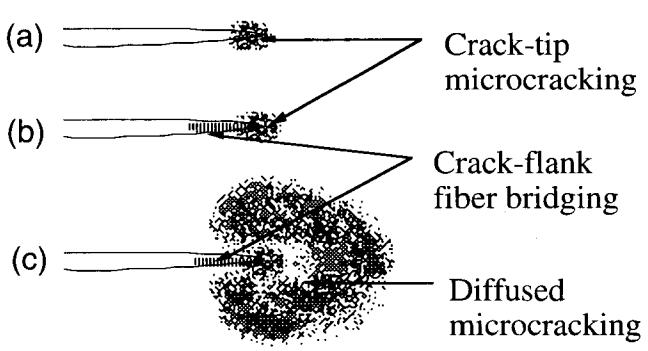

Fig. 1. Fracture process zone in (a) brittle cement, (b) quasi-brittle concrete and FRC, and (c) ductile ECC.

A. G. Evans—contributing editor

Manuscript No. 193785. Received February 28, 1994; approved September 30, 1994.

Supported in part by Grant No. BCS 9202097 from the National Science Foundation to the University of Michigan. A U-M Rackham Predoctoral Fellowship Award supported the Ph.D. study of M. Maalej.

*Member, American Ceramic Society.

program includes testing of uniaxial tension specimens to determine J_b and DCB specimens to determine J_c. The total fracture energy is determined by means of the J-based technique,[9] using a set of DCB specimens with different notch lengths. The off-crack-plane energy J_m is then deduced from the difference between J_c and J_b.

II. Brief Description of the J-Based Technique

This section provides the principle of the J-based technique. According to Rice,[10] the path-independent integral defined as

$$J = \int_{\Gamma} \left(W \, dy - T_i \frac{\partial u_i}{\partial x} ds \right) \tag{1}$$

where W is the elastic strain energy density, T_i is the traction vector, u_i is the displacement vector, Γ is a closed contour followed counterclockwise in a stressed solid, and ds is an element of Γ (see Fig. 2(a)), may be interpreted as the change in potential energy for a virtual crack extension:

$$J = -\frac{\partial U}{\partial a} \tag{2}$$

where U is the potential energy and a is the crack length. U can be obtained from a global load deformation curve; therefore, by the use of Eq. (2), J can be determined. As an example, consider a DCB specimen loaded with a load level P, and a load point displacement Δ (see Fig. 2(b)). Equation (2) implies

$$J(\Delta) = -\frac{1}{B} \int_0^{\Delta} \left(\frac{\partial P}{\partial a} \right)_{\Delta'} d\Delta' \tag{3}$$

However, since crack tip positions are difficult to locate accurately, it would be almost impossible to directly evaluate Eq. (3) by propagating a crack in a single specimen. An alternative and approximate procedure is to use two identical DCB specimens with different notch lengths a_1 and a_2. In this case, the integral in Eq. (3) may be interpreted as the area between the P–Δ curves for each of the two specimens divided by the difference in notch length, i.e.,

$$J(\Delta) = \frac{1}{B} \frac{\text{Area}(\Delta)}{a_2 - a_1} \tag{4}$$

It is expected that $J(\Delta)$ increases from zero and asymptotically approaches a steady-state value J_c. When J_c is reached in a quasi-brittle material, a bridging process zone would have fully developed. When J_c is reached in an ECC material, a bridging process zone and an off-crack-plane damage zone would have fully developed. Further crack propagation can then be viewed as a simple translation of these inelastic process zones along the plane of the crack. In terms of an R-curve behavior, J_c would correspond to the plateau value of the R–Δa curve.

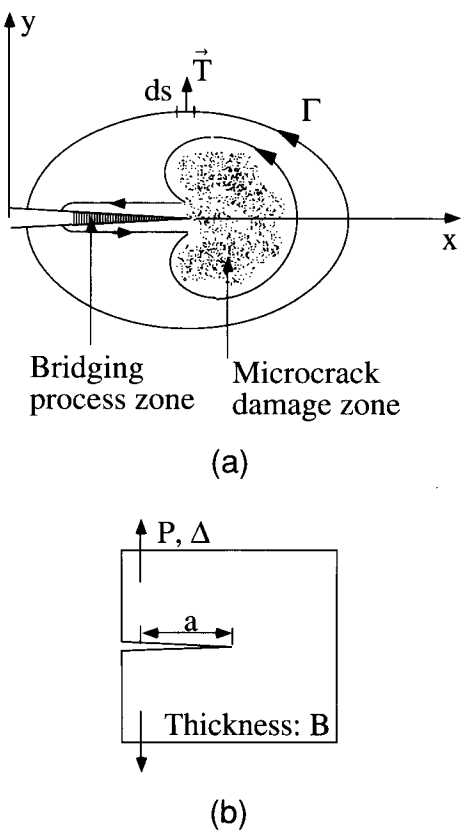

Fig. 2. (a) J-integral contours around crack tip, (b) DCB fracture specimen.

III. Experimental Program

(1) *Materials and Specimen Configurations*

The material selected for testing was a polyethylene-fiber-reinforced cement. The constituent materials used and their mix proportions are given in Table I. Type I portland cement was used to form the matrix of the composite. The fiber length and diameter were 12.7 mm and 38 μm, respectively. To study the effect of fiber volume fraction on the off-crack-plane fracture energy, uniaxial tension (UT), and fracture (DCB), specimens with different fiber contents, ranging from 0.2% to 4%, were prepared. The configurations and dimensions of the prepared specimens are shown in Fig. 3 and Table II, respectively. It should be noted here that as steady-state crack growth was not observed by Li and Hashida[1] on the 2% polyethylene fiber composite using the medium size DCB specimen, larger size DCB specimens were used in this program to measure the steady-state total fracture energy J_c for composites where the fiber volume fraction is equal to 2%, 3%, and 4%.

(2) *Specimen Preparation*

The polyethylene fibers are supplied from the manufacturer in bundlelike form. Prior to mixing, the fibers were dispersed using air pressure for approximately 1 min. Then the amount of fiber needed for the mix was weighed. After measuring the weight of all mix constituents, the cement was poured into a

Table I. Matrix Mix Proportions (by Weight)

Materials	Cement	Silica fume	Superplasticizer	Water
Mix proportions	1.0	0.10	0.01	0.27

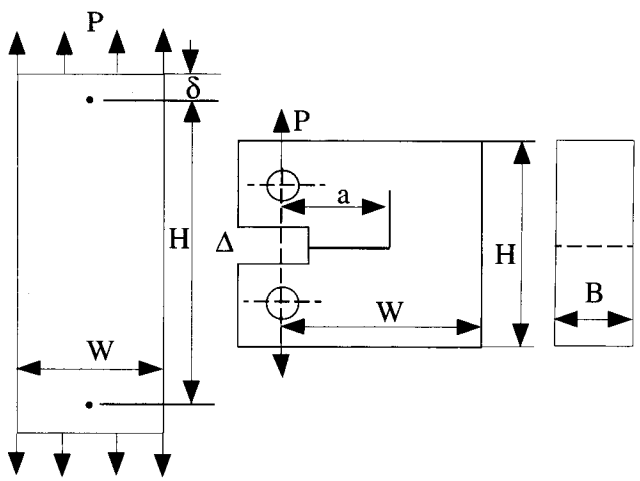

Fig. 3. Specimen configurations used.

Table II. Geometry of Fracture and UT Specimens

Specimen	*W* (mm)	*H* (mm)	*B* (mm)
Small DCB	127	153	35
Medium DCB	310	300	35
Large DCB	490	585	35
UT	76	207	13

three-speed (Hobart) mixer with a planetary rotating blade. After starting the mixer, the silica fume was slowly added to the cement. Then water and superplasticizer were mixed together and slowly added. When all water and superplasticizer were added and the cement paste mix became uniform, the dispersed fibers were slowly added by hand to the mix. The total mixing time ranged between 15 and 30 min, depending on the batch size and the amount of fiber used (fiber volume fraction). Note that the workability of the 3% and 4% (in particular) fiber composites was not as good as that for the lower fiber volume fraction composites. When the mix was ready, the specimens were cast under high-frequency vibration (150 Hz) in already greased Plexiglass molds. After casting, they were covered with a polyethylene sheet and allowed to harden at room temperature for 1 day prior to demolding. After demolding, the specimens were placed in a water curing tank for 4 weeks. Subsequently they were removed from water and prepared for testing. A thin white coating of lime was applied on the specimens prior to testing to better monitor the development of cracks. The age of the specimens at testing was 30 to 60 days.

(3) Testing Procedure

The uniaxial tensile specimens were tested under displacement control in a 133.5 kN capacity MTS 810 material-testing system with hydraulic wedge grips. Aluminum plates were glued onto the ends of the tension specimens to facilitate gripping. Care was taken to ensure proper alignment of the specimens with the machine hydraulic grips. The MTS machine has a fully digital control panel and Teststar software to automatically run the tests and collect the load and actuator displacement data. In addition, two linear variable differential transducers (LVDTs) connected to a data acquisition system were used to measure the relative displacement between the two points on the specimen surface (see Fig. 3). The gage length for the measurement was approximately 207 mm. The data acquisition system consisted of a Schaevitz LVDT signal conditioner and Labtech Notebook software.

The fracture toughness tests were conducted in the same MTS testing system as the UT tests. A clevis and pin arrangement (similar to that recommended by ASTM E399-78) was employed at both the top and bottom of the DCB specimens to allow rotation as the specimens were loaded. The specimens were loaded to complete failure with a constant crosshead speed; the testing time was typically 40 min for each test. The load-line displacement Δ was measured using two LVDTs. Concurrently with the tests, damage evolution on the specimen surface was recorded, using a camera.

IV. Results and Discussion

The purpose of the small DCB specimens is to measure the elastic modulus and fracture toughness of the cement matrix. These are used in predicting the critical fiber volume fraction needed for the polyethylene fiber composite to exhibit pseudo-strain-hardening behavior. These specimens yielded an average matrix elastic modulus and fracture toughness of 13.6 GPa and 0.33 MPa·m$^{1/2}$, respectively. The elastic modulus was determined by the compliance method, and the K_{IC} of the cement paste was measured following the ASTM E399-78 testing procedure. The dimensionless specimen compliance formula for the DCB specimens was taken from Newman's boundary collocation analysis.[11] Because of its homogeneity and rather brittle behavior, hardened cement paste can be viewed as a model material concerning the application of linear elastic fracture mechanics to cementitious materials. This point was experimentally confirmed by Mindess *et al.*[12] Therefore, the K_{IC} measurement of the cement paste matrix should be fairly accurate.

Examination of the pseudo-strain-hardening conditions as outlined by Li[8] indicated that this polyethylene fiber composite can exhibit pseudo-strain-hardening behavior if the fiber volume fraction is greater than about 0.6%–0.8%. This estimate is based on a fiber/matrix interface bond strength of 0.7–0.8 MPa and a snubbing factor of 2.1 (this factor accounts for a local frictional effect, called snubbing, resulting from the misalignment between the axis of a fiber bridging a matrix crack and the loading axis[13]). The bond strength has been experimentally measured by a single-fiber pull-out test[14] and from inference from ultimate tensile strength and is known to depend on age, matrix composition, and even fiber volume fraction. The snubbing factor has not been measured for this material system, although polypropylene and nylon fibers in cementitious systems show snubbing factors of 1.8 and 2.3, respectively.[13] The above discussion means that the 0.2% and 0.4% fiber composites are expected to exhibit quasi-brittle behavior, while the 0.8%, 1%, 2%, 3%, and 4% fiber composites are expected to exhibit pseudo-strain-hardening behavior. As it will be shown later, this was found to be the case.

Figure 4 shows a comparison between two stress–deformation curves recorded on uniaxial tension specimens. The first, corresponding to the 2% fiber composite, shows a clear pseudo-strain-hardening behavior with an average strain at peak stress approximately equal to 6% (about 600 times the strain capacity of the unreinforced matrix). For this composite, real-time observation showed that multiple cracking occurred with many subparallel cracks across the specimen during strain-hardening. Beyond peak stress, localized crack extension occurred accompanied by fiber bridging. The second, corresponding to the 0.4% fiber composite, shows a behavior similar to that of quasi-brittle material. After first cracking, the specimen failed by a decaying bridging stesss. In either case, the fracture energy J_b due to fiber bridging may be computed by integrating the post-peak stress–displacement relation.

Figures 5 and 6 show an example of stress–deformation and damage record for a uniaxial tension specimen. As indicated in these figures, although the specimen is already cracked at stage (a), the material continues to sustain the applied load. At stage (b) more cracks have developed in the specimen, but the material is still capable of resisting higher levels of loading. As further deformation is imposed on the specimen, further cracking takes place (stage (c)). At stage (d), a single macrocrack has already localized in the specimen and the material has started to soften. The actual macrocrack was not recorded, but it has

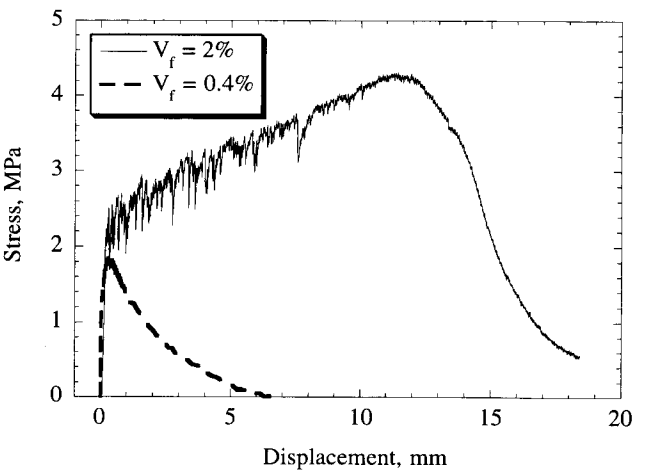

Fig. 4. Comparison between the UT stress–deformation response of a quasi-brittle material and that of a strain-hardening material.

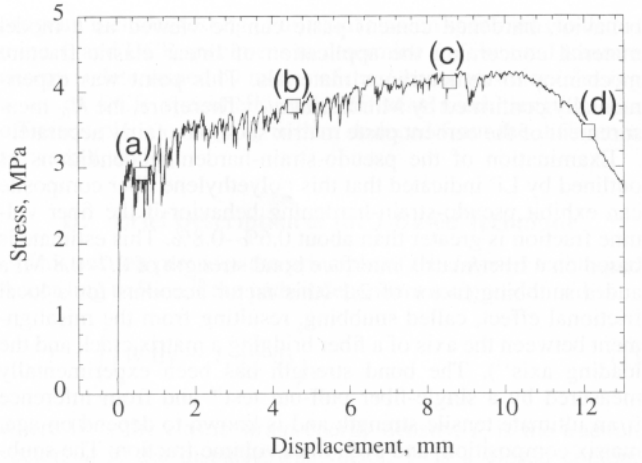

Fig. 5. UT stress–deformation record.

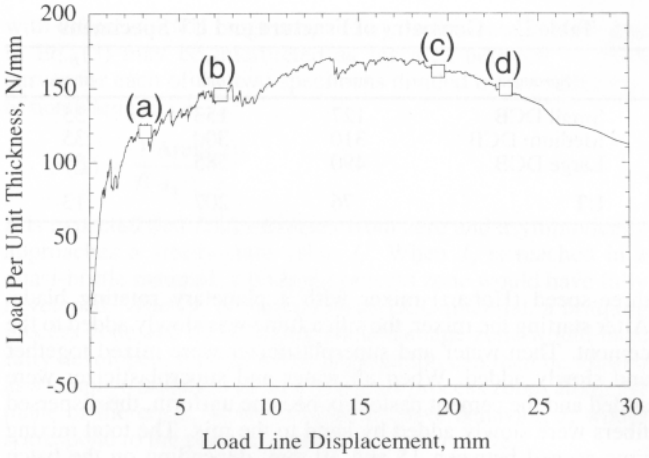

Fig. 7. DCB load–displacement record.

occurred in a location close to the one shown on the left side of Fig. 6(d).

Figure 7 shows an example of a load–displacement curve recorded for a large DCB fracture specimen. It is seen that, despite the presence of the deep notch, the material produces significant damage tolerance subsequent to the bendover point. Figure 8 presents the damage evolution recorded for various load-line deformation values indicated in Fig. 7. It is particularly noted that an extensive microcrack damage zone spreads around the notch tip before the localized crack starts to grow. Significant energy absorption is therefore expected from the off-crack-plane volumetric inelastic process.

In order to illustrate the data analysis procedure of the *J*-based technique, used in this paper to determine the total fracture energy J_c of the different materials, a set of experimental results for the 2% polyethylene fiber composite is presented first. Figure 9 shows load–displacement records for two DCB specimens with different notch lengths. The total fracture energy J_c can be evaluated by the use of Eq. (4):

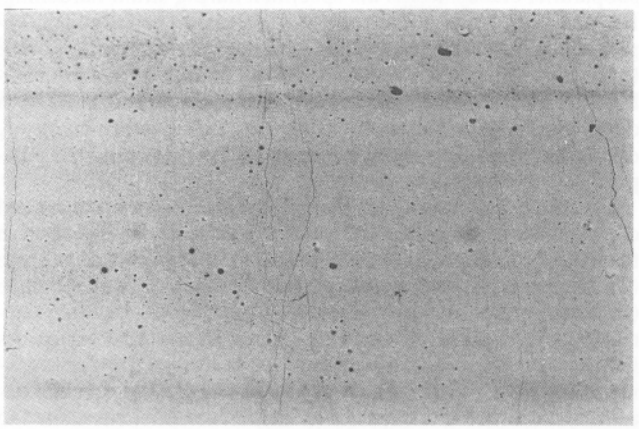

(a)

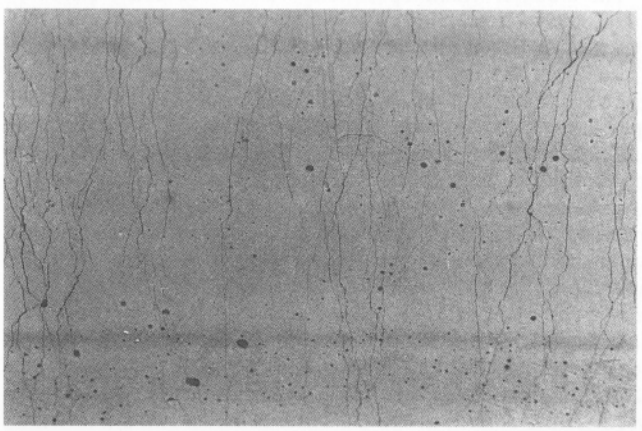

(b)

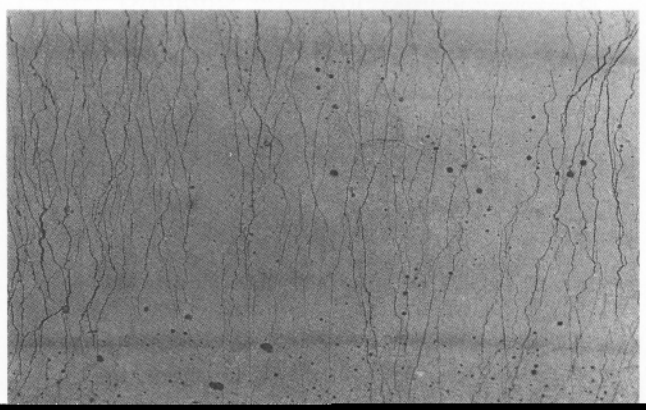

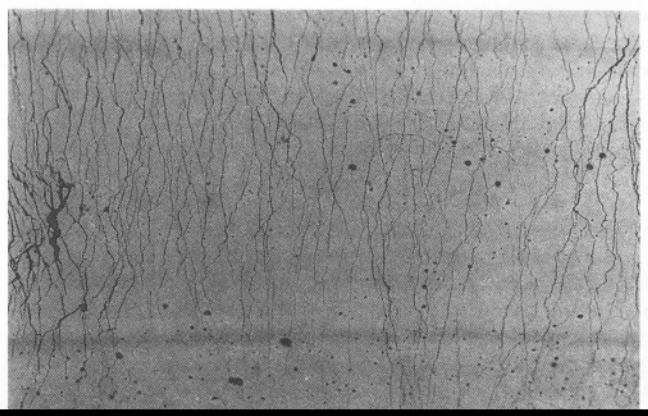

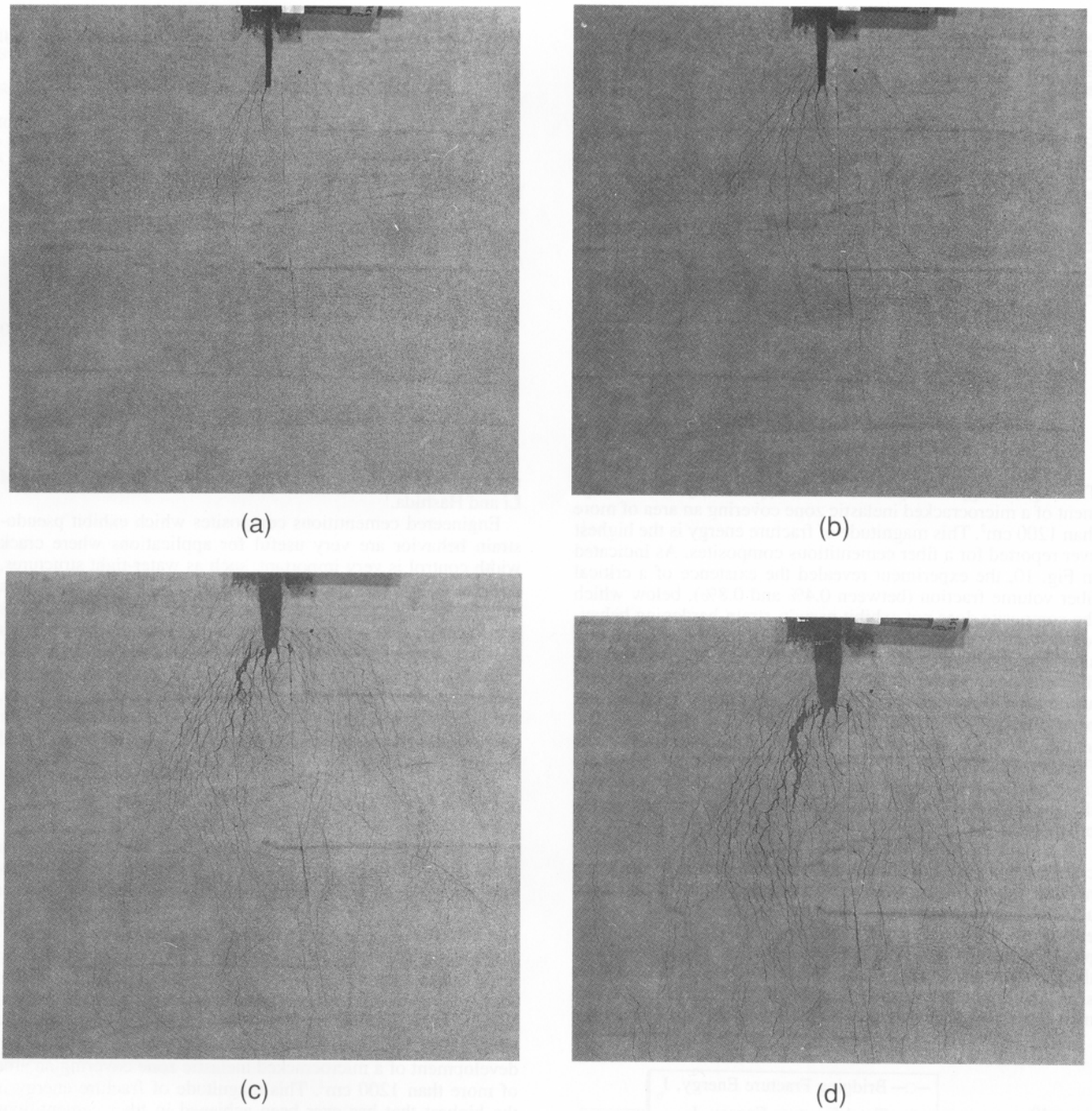

Fig. 8. DCB damage evolution as a function of deformation: (a) $\Delta = 3.10$ mm, (b) $\Delta = 7.32$ mm, (c) $\Delta = 19.45$ mm, (d) $\Delta = 23.16$ mm.

$$J_c = J(\Delta_c) = \frac{1}{B}\frac{\text{Area}(\Delta_c)}{(a_2 - a_1)} = \frac{1}{(a_2 - a_1)}\int_0^{\Delta_c}\left(\frac{P_1}{B_1} - \frac{P_2}{B_2}\right)d\Delta$$

$$= \frac{S}{(a_2 - a_1)} \tag{5}$$

where subscripts 1 and 2 refer to the two different notch lengths, B is the specimen thickness, Δ_c is the load line displacement at which the two $P/B - \Delta$ curves meet, and S is the area between $P/B - \Delta$ curves of the two specimens, as exemplified in Fig. 9. The measured total fracture energy J_c can be interpreted as the total energy flux provided by the applied load and elastic strain energy release and must therefore be equal to the sum of the bridging fracture energy J_b, and the off-crack-plane fracture energy J_m.[1] Thus, the fracture energy contribution J_m from the off-crack-plane microcracking may be obtained from the difference between the J_c and J_b.

The above procedure is repeated for the other fiber composites. The results are summarized in Fig. 10, which shows the total fracture energy J_c and the bridging fracture energy J_b plotted against the fiber volume fraction. In this figure, the numbers in brackets indicate the maximum size of the inelastic microcracked zone in units of cm^2. Figure 10 shows that J_c and J_b increase with increasing V_f. Initially, the relationship is almost linear, but then deviates from linearity and shows a saturation behavior. This behavior is probably related to bond deterioration at high fiber volume fractions due to fiber interaction. This bond deterioration phenomenon, also observed in steel fiber composites,[5] is currently under investigation at the University of Michigan. It can be deduced from Fig. 10 that the off-crack-plane fracture energy increases with increasing fiber volume fractions, and it is slightly higher than the bridging fracture energy. Furthermore, we can see that the total fracture energy, measured on the 4% fiber composite, is about 34 kJ/m^2.

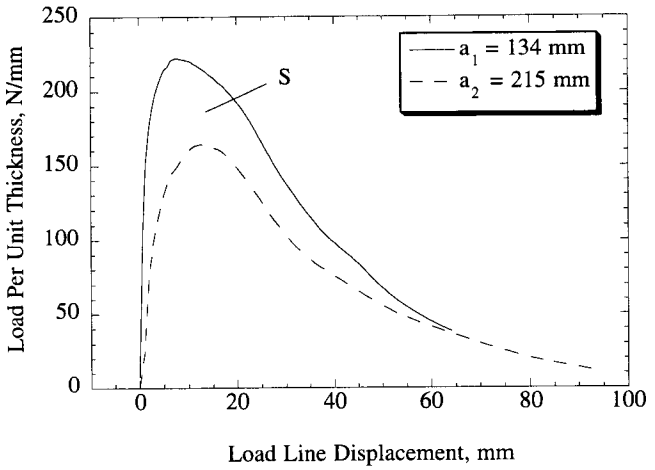

Fig. 9. DCB load–displacement records for J-based method.

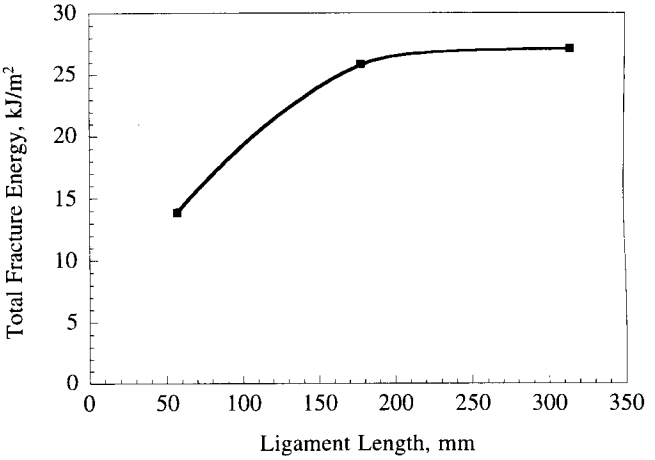

Fig. 11. Effect of specimen size on the total fracture energy J_c.

This high energy absorption was accompanied by the development of a microcracked inelastic zone covering an area of more than 1200 cm^2. This magnitude of fracture energy is the highest ever reported for a fiber cementitious composites. As indicated in Fig. 10, the experiment revealed the existence of a critical fiber volume fraction (between 0.4% and 0.8%), below which the composite does not exhibit pseudo-strain-hardening behavior. Overall, there was a consistency between the uniaxial tension tests and the fracture tests. The 0.8%, 1%, 2%, 3%, and 4% fiber composites have shown multiple cracking on both the UT and the DCB specimens. However, no multiple cracking has been observed on any of the specimens made from the 0.2% and 0.4% fiber composites. This result is consistent with Fig. 10, which shows no J_m component for the 0.2% and 0.4% fiber composites. It is also consistent with the earlier prediction that the 0.2% and 0.4% fiber composites should exhibit a quasi-brittle behavior.

It should be noted that, in all DCB specimens, the microcracking zone did not spread up to the dimension of the beam height. This confirms that steady-state crack growth has been achieved in all specimens and the measured total fracture energy reflects steady-state conditions. For the 2% fiber composite, this point is further supported by Fig. 11, which shows the total fracture energy J_c plotted as a function of specimen size. The ligament length is selected as a representative specimen dimension. The data points corresponding to the small and medium size DCB specimens are taken from the initial study of Li and Hashida.[1]

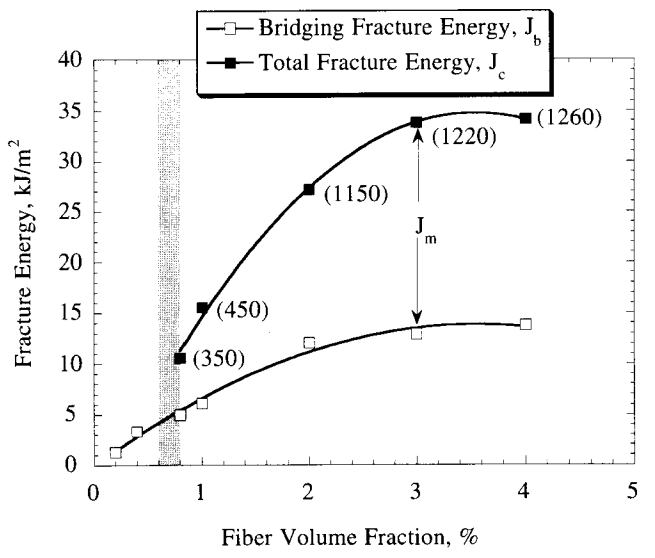

Fig. 10. Effect of fiber volume fraction on J_c and J_b. The estimated critical fiber volume fraction is indicated by the shaded strip.

Engineered cementitious composites which exhibit pseudo-strain behavior are very useful for applications where crack width control is very important, such as water-tight structures, water and sewage pipes, or even bridges where water is a vehicle for aggressive agents that can attack concrete and/or its reinforcement. In addition, the strain-hardening behavior gives ECCs a significant advantage under flexural loading. In a three-point bending test, Maalej and Li[15] found the flexural strength of an ECC to be five times its tensile (first cracking) strength. Note that the ratio of flexural strength to tensile strength for quasi-brittle materials, such as regular FRC, has an upper bound of three.

V. Conclusions

In this paper, an experimental study has been conducted on the effect of fiber volume fraction on the off-crack-plane fracture energy in a strain-hardening polyethylene-fiber–cement composite. The fiber volume fraction was varied between 0.2% and 4%. The experiment showed that the off-crack-plane fracture energy increases with increasing fiber volume fractions in a logarithmic fashion, and it can exceed the bridging fracture energy on the main fracture plane. In addition, the total fracture energy, measured on the 4% fiber composite, was about 34 kJ/m^2. This high energy absorption was accompanied by the development of a microcracked inelastic zone covering an area of more than 1200 cm^2. This magnitude of fracture energy is the highest that has ever been achieved in fiber cementitious composites. Moreover, the experiment revealed the existence of a critical fiber volume fraction (between 0.4% and 0.8%), below which the composite does not exhibit the damage-tolerant behavior. Finally, these experiments, together with those of Li and Hashida,[1] demonstrate that high damage tolerance can be built into brittle matrix composites. The experience of the present work can be transferred to other fiber and brittle matrix types.

References

[1]V. C. Li and T. Hashida, "Engineering Ductile Fracture in Brittle Matrix Composites," *J. Mater. Sci. Lett.*, **12**, 898–901 (1993).

[2]J. Aveston, R. A. Mercer, and J. M. Sillwood, "Fiber Reinforced Cements—Scientific Foundations for Specifications"; pp. 93–103 in *Composites Standards Testing and Design*. IPC Science and Technology Press, Guildford, U.K., 1974.

[3]H. Krenchel and H. Stang, "Stable Microcracking in Cementitious Materials"; pp. 20–33 in *Proceedings of the Second International Symposium on Brittle Matrix Composites—BMC 2*. Edited by A. M. Brandt and I. H. Marshall. Cedzyna, Poland, 1988.

[4]V. C. Li and H. C. Wu, "Micromechanics Based Design for Pseudo Strain-Hardening in Cementitious Composites"; pp. 740–43 in *Engineering Mechanics*. Edited by L. D. Lutes and J. M. Niedzwecki. American Society of Civil Engineers, New York, 1992.

[5]V. C. Li, H. C. Wu, M. Maalej, D. K. Mishra, and T. Hashida, "Tensile Behavior of Engineered Cementitious Composites with Discontinuous Random Steel Fibers," *J. Am. Ceram. Soc.*, in press.

[6]V. C. Li and C. K. Y. Leung, "Steady State and Multiple Cracking of Short Random Fiber Composites," *J. Eng. Mech.*, **118** [11] 2246–64 (1992).

[7]V. C. Li and H. C. Wu, "Conditions for Pseudo Strain-Hardening in Fiber Reinforced Brittle Matrix Composites," *Appl. Mech. Rev.*, **45** [8] 390–98 (1992).

[8]V. C. Li, "From Micromechanics to Structural Engineering—the Design of Cementitious Composites for Civil Engineering Applications," *ASCE J. Struct. Mech. Earthquake Eng.*, **10** [2] 37–48 (1993).

[9]V. C. Li, C. M. Chan, and C. K. Y. Leung, "Experimental Determination of the Tension–Softening Curve in Cementitious Composites," *Cem. Concr. Res.*, **17** [3] 441–52 (1987).

[10]J. R. Rice, "Mathematical Analysis in the Mechanics of Fracture"; pp. 191 in *Fracture: An Advanced Treatise*, Vol. 2. Edited by H. Liebowitz. Academic Press, New York, 1968.

[11]J. C. Newman Jr., "Stress Analysis of the Compact Specimen Including the Effects of Pin Loading"; pp. 105–21 in *Proceedings of the 1973 National Symposium, on Fracture Mechanics, Part II*, ASTM STP 560. American Society for Testing and Materials, Philadelphia, PA, 1974.

[12]S. Mindess, F. V. Lawrence, and C. E. Kesler, "The *J*-integral as a Fracture Criterion for Fiber Reinforced Concrete," *Cem. Concr. Res.*, **7**, 731–42 (1977).

[13]V. C. Li, Y. Wang, and S. Backer, "Effect of Inclining Angle, Bundling, and Surface Treatment on Synthetic Fiber Pull-Out from a Cement Matrix," *J. Compos.*, **21** [2] 132–40 (1990).

[14]V. C. Li, H. C. Wu, and Y. W. Chan, "Interfacial Property Tailoring for Pseudo-Strain Hardening Cementitious Composites"; pp. 261–68 in *Advanced Technology on Design and Fabrication of Composite Materials and Structures*. Edited by Carpinteri and Sih. Kluwer Academic Publishers, Dordrecht, Netherlands, 1995.

[15]M. Maalej and V. C. Li, "Flexural/Tensile Strength Ratio in Engineered Cementitious Composites," *ASCE J. Mater. Civ. Eng.*, in press. □